Aug 24th, 12:00 AM - Aug 25th, 12:00 AM

Compressive Strength Tests and Design of Cold-formed Plain and Dimpled Steel Columns

V. B. Nquyen

C. J. Wang

D. J. Mynors

M. A. English

M. A. Castellucci

Twenty-First International Specialty Conference on Cold-Formed Steel Structures
St. Louis, Missouri, USA, October 24 & 25, 2012

Compressive strength tests and design of cold-formed plain and dimpled steel columns

V.B. Nguyen[1], C.J. Wang[2], D.J. Mynors[3], M.A. English[4] and M.A. Castellucci[5]

Abstract

This paper presents the experiments and design formulae of cold-formed plain and dimpled steel columns. A series of compression tests on plain and dimpled channel columns were conducted over a range of different geometries and the strength of the columns were investigated. The change in strength of the dimpled columns resulting from the cold working associated with the dimpling process was considered. The results showed that the buckling and ultimate strengths of dimpled steel columns were up to 33% and 26% greater than plain steel columns, respectively. The test results were evaluated by comparing buckling and ultimate loads of plain and dimpled channel columns with the values predicted by theoretical and semi-empirical methods. It was found that the predicted buckling and ultimate loads correlated well with the experimental results. Based on the experimental results, expressions for determining buckling and ultimate strengths of component plate elements of plain and dimpled channel columns were formulated.

[1]Research Engineer, Hadley Industries plc, Smethwick, West Midlands, UK and University of Wolverhampton, Wolverhampton, West Midlands, UK.
[2]Senior Lecturer, University of Wolverhampton, Wolverhampton, West Midlands, UK.
[3]Professor and Head of Department of Engineering, University of Wolverhampton, Wolverhampton, West Midlands, UK.
[4]Design and Development Manager, Hadley Industries plc, Smethwick, West Midlands, UK.
[5]Technical Director, Hadley Industries plc, Smethwick, West Midlands, UK.

Introduction

The UltraSTEEL® dimpling process developed by Hadley Industries plc is a method to impart cold work to the whole sheet and thus significantly improve the material and structural performance by extending the regions of work hardening (Nguyen et al. 2011). The process uses a pair of rolls which are designed with rows of specially shaped teeth that stretch the surface forming the dimple shapes from both sides of the plain sheet. The dimpled sheet can then be progressively formed into a desired product by passing it through a series of rolls, arranged in tandem, or by press braking. The effect of the dimpling process on the mechanical and structural properties of the steel material has been the subject of recent experimental investigations through micro-hardness, tensile, bending and compression tests of plain and dimpled steel specimens (Collins et al. 2004, Nguyen et al. 2011, 2012). It showed that the strengths of dimpled specimens were significantly greater than plain specimens - caused by the cold work of the material during the dimpling process. In addition, finite element analysis (Nguyen et al. 2011) has shown plastic strains are developed throughout the entire thickness of the dimpled steel sheet which could be attributable to the increase in strength recorded in experimental tests.

UltraSTEEL® dimpled steel products are increasingly used in a wide range of applications, including wall studs, framing and roofing members, corrugated panels, vineyard posts, windows and door reinforcement and many other products. The wider use of cold-formed dimpled steel members has promoted considerable interest in the local instability and strength of these members. Of particular interest is their buckling behaviour and ultimate strength capacity. Recent design specifications for cold-formed steel provide design criteria for compressive strength of cold-formed plain steel members. However, design criteria for compressive strength of such cold-formed dimpled steel members have not been available. In a recent study (Nguyen et al. 2012), compression tests of cold-formed plain and dimpled steel columns of different geometries were conducted. This enables the test data for evaluation and establishing design procedures for cold-formed dimpled steel.

The objectives of this paper are to investigate the compressive strength of cold-formed plain and dimpled steel columns and to propose design expressions for the columns. The ‘short’ plain and dimpled channel columns were tested in purely axial compression, fixed at both ends. The test data reported previously (Nguyen et al. 2012) and data from tests carried out more recently have been summarised. All the test results were then evaluated by comparing the buckling and ultimate loads with the predicted values based on theoretical and semi-

empirical methods. Finally, the experimental results presented here were used to formulate design expressions for determining the compressive strength of component elements of cold-formed plain and dimpled steel columns.

Summary of the test programme

The test program described in Nguyen et al. (2012) and tests carried out more recently provided buckling and ultimate loads and failure modes for the plain and dimpled columns. The channel specimens were selected for a range of different geometries (lengths and cross sections) and fabricated by both cold-rolled forming and press-braking. Measured test section geometries and dimensions are given in Table 1.

The specimens were organised into 11 groups of b_f/b_w ratios ranging from 0.28 to 1.95, in which b_f is the width of the flange excluding the corner radius and b_w is the width of the web excluding the corner radii. Each group contains four column specimens. Test groups 2−4 and 7−11 contain plain and dimpled specimens originating from the same coil of material, fabricating by the same forming method and having the same nominal dimensions. Test groups 1, 5, 6 contain only plain specimens. Data of the test groups 2, 3, 4, 7, 8 and 11 were extracted from Nguyen et al. (2012). The column specimens were labelled, a plain specimen label starts with the letter 'P' whilst a dimpled specimen starts with the letter 'U'; and #1: The first specimen (if a test was repeated, then #2, #3, and #4 indicating the second, third and fourth specimens, respectively). The material properties were determined from tensile tests of plain and dimpled specimens. Details of the tensile test procedure and results were provided in Nguyen et al. (2011, 2012).

A compressive axial force was applied to the column specimen by using a 200 kN capacity test rig. A detailed test programme that related to the arrangement of strain gauges and displacement transducers (LVDTs), specimen calibration, measurements, test setup, support end conditions, alignment procedure, instrumentation for determining buckling load and test procedure was described in Nguyen et al. (2012).

Determination of the buckling load

Experimental buckling load

For plain column specimens, the experimental critical buckling load was determined from the strain gauge readings using the vertical tangent method (Forest Products Laboratory 1946).

Table 1 Measured test section geometries and dimensions. * Data given in Nguyen et al. (2012)

Test group (1)	Specimen (2)	Thickness t (mm) (3)	Width b (mm) (4)	Depth d (mm) (5)	Radius r (mm) (6)	Length L (mm) (7)	Area A (mm^2) (8)
1	P-T1.5F29.6W101.6L500#1	1.49	29.76	101.04	0.80	499.76	232.16
	P-T1.5F29.6W101.6L500#2	1.49	29.53	101.04	0.80	499.46	231.58
	P-T1.5F29.6W101.6L500#3	1.49	29.65	101.03	0.80	499.81	231.86
	P-T1.5F29.6W101.6L500#4	1.49	29.65	101.04	0.80	499.95	231.88
2*	P-T0.9F15.0W44.7L200						
	U-T0.9F15.0W44.7L200						
3*	P-T1.5F30.4W70.0L500						
	U-T1.5F30.4W70.0L500						
4*	P-T1.0F50.8W101.6L500						
	U-T1.0F50.8W101.6L500						
5	P-T0.8F31.0W51.7L200#1	0.79	31.24	51.56	1.50	199.74	87.67
	P-T0.8F31.0W51.7L200#2	0.79	31.22	51.60	1.50	200.09	87.85
	P-T0.8F31.0W51.7L200#3	0.78	31.20	51.58	1.50	199.77	86.42
	P-T0.8F31.0W51.7L200#4	0.79	31.22	51.58	1.50	199.67	87.31
6	P-T0.8F38.0W51.7L200#1	0.79	38.28	51.71	1.50	199.59	98.91
	P-T0.8F38.0W51.7L200#2	0.79	38.40	51.66	1.50	199.86	99.03
	P-T0.8F38.0W51.7L200#3	0.79	38.21	51.67	1.50	199.65	98.73
	P-T0.8F38.0W51.7L200#4	0.79	38.30	51.68	1.50	199.78	98.89
7*	P-T1.2F24.5W32.0L200						
	U-T1.2F24.5W32.0L200						
8*	P-T1.2F32.5W32.0L400						
	U-T1.2F32.5W32.0L400						
9	P-T1.2F38.0W32.0L400#1	1.15	39.29	31.80	1.20	399.80	122.56
	P-T1.2F38.0W32.0L400#2	1.16	38.86	32.00	1.20	399.77	123.02
	P-T1.2F38.0W32.0L400#3	1.15	39.32	31.96	1.20	399.91	123.00
	P-T1.2F38.0W32.0L400#4	1.15	39.16	31.92	1.20	399.83	122.86
	U-T1.2F38.0W32.0L400#1	1.09	38.56	31.83	1.20	400.09	120.89
	U-T1.2F38.0W32.0L400#2	1.12	38.43	31.81	1.20	399.55	120.56
	U-T1.2F38.0W32.0L400#3	1.11	38.66	31.79	1.20	399.68	121.08
	U-T1.2F38.0W32.0L400#4	1.10	38.51	31.84	1.20	399.95	121.79
10	P-T1.2F46.0W32.0L400#1	1.15	46.84	31.80	1.20	399.63	139.94
	P-T1.2F46.0W32.0L400#2	1.15	46.35	31.99	1.20	399.76	138.75
	P-T1.2F46.0W32.0L400#3	1.15	47.00	31.98	1.20	399.65	140.52
	P-T1.2F46.0W32.0L400#4	1.15	46.73	31.92	1.20	399.68	139.74
	U-T1.2F46.0W32.0L400#1	1.10	46.86	31.76	1.20	399.71	139.66
	U-T1.2F46.0W32.0L400#2	1.01	46.78	31.84	1.20	399.80	139.57
	U-T1.2F46.0W32.0L400#3	1.03	46.96	31.84	1.20	399.54	140.25
	U-T1.2F46.0W32.0L400#4	1.04	46.60	31.80	1.20	399.33	139.39
11*	P-T1.2F55.0W32.0L500						
	U-T1.2F55.0W32.0L500						

For dimpled column specimens, it was determined from the LVDTs data by plotting the load P against the out-of-plane displacement w (Coan 1951, Venkatatamaiah and Rooda 1982), as shown in Nguyen et al. (2012). For evaluation, special strain gauges (Model EA-06-015LA-120, Vishay Precision Group) were used in the dimpled column specimen as shown in the test setup in Figure 1. They included a small strain gauge with an overall length less than 0.25 mm, and a long strain gauge with an overall length of 60 mm. They were mounted on the specimen mid-height, at the centres of the web. The small gauge is fixed to the valley surface of one dimple, inside the specimen section, to measure the local strain at the dimple; the long gauge is attached over a number of dimples, outside the specimen section, to measure the average strain of the column. Figure 2 illustrates the results obtained from a dimpled column specimen (U-T1.0F50.8W101.6L500#2, test group 4) in which the critical buckling loads determined by LVDTs and strain gauges data are also presented. It clearly shows that the critical buckling load determined from LVDT data are similar to those of strain gauges readings. Thus, LVDTs were used for determining the critical buckling load in dimpled column specimens.

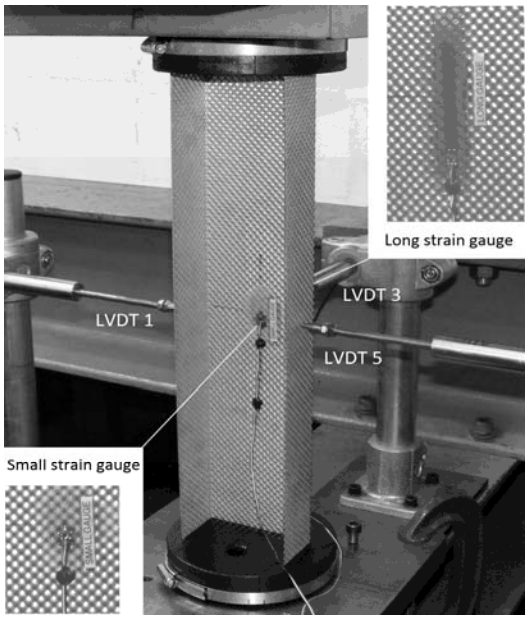

Figure 1 Experimental setup of the dimpled column specimen with the attached strain gauges

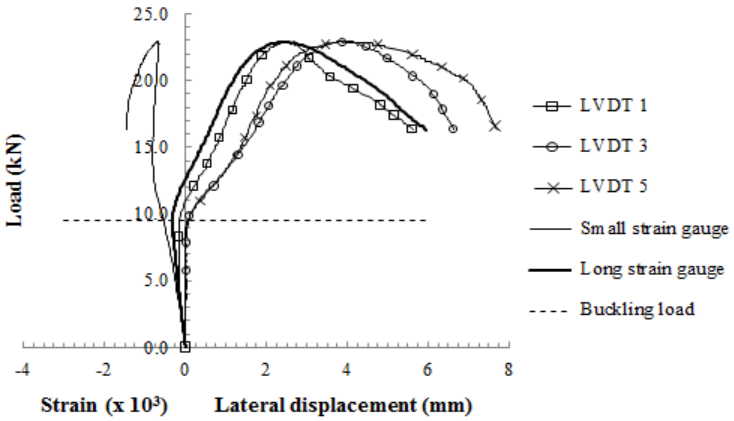

Figure 2 Load−out-of-plane displacement and load−strain curves of a dimpled column specimen (U-T1.0F50.8W101.6L500#2, test group 4)

In this study, buckling of column specimens was derived on the two approaches: buckling of a complete section and buckling of component elements. In the latter, a plain channel column's section could be considered as consisting of individual flat plate elements: web and flange elements. Local buckling in the web and flange elements was indicated using the vertical tangent method, as described previously. The critical buckling strains in the web element ε_{crw} and in the flange element ε_{crf} were experimentally determined (the point on their P-ε curves at which the rate of strain decreases rapidly). Therefore, the buckling coefficients of the web element k_w and the flange element k_f were calculated from the following equations (Bulson 1970):

$$k_w = [12P_{crw}(1 - \nu^2)(b_w/t)^2]/\pi^2 EA_w \quad (1)$$

$$k_f = [12P_{crf}(1 - \nu^2)(b_f/t)^2]/\pi^2 EA_f \quad (2)$$

Where P_{crw} (= $\varepsilon_{crw}EA_w$) and P_{crf} (= ε_{crf} EA_f) are the experimental critical buckling loads in the web and flange elements, respectively; A_w and A_f are the sectional areas of the web and flange elements, respectively; E is the Young's modulus; ν is the Poisson's ratio; b_w and b_f are the widths of the web and flange elements, respectively, and t is the thickness of the section.

The equations (1) and (2) are applicable for plain sections. For dimpled column specimens, local buckling in the web and flange elements was indicated using the method based on LVDTs data, as described previously. The critical buckling strains in the web and flange elements, however, were generally not known. It was therefore assumed that the distribution of the critical buckling loads of the web or flange elements on the cross section of the dimpled column is similar to that of the plain column from the same test group. In other words, the

assumption could be expressed that, for buckling of web elements, the ratio $\beta_w = P_{crw}/P_{cr}$ of a dimpled column is equal to the ratio $\beta_w = P_{crw}/P_{cr}$ of a plain column, in the same test group. $\beta_w = P_{crw}/P_{cr}$ of a plain column was obtained, in which $P_{crw} = \varepsilon_{crw}EA_w$ is the experimental buckling load of the web element and P_{cr} is the critical buckling of the plain column, determined from tests. β_w of a dimpled column was deemed to be *the average of* P_{crw}/P_{cr} *of all plain columns in the same test group* (β_{wd}), in order to take into account the variation of P_{crw}/P_{cr} for different plain columns in the same test group. Similarly, for buckling of flange elements, β_f of a dimpled column specimen was deemed to be *the average of* P_{crf}/P_{cr} *of all plain column specimens in the same test group* (β_{fd}); where $P_{crf} = \varepsilon_{crf}EA_f$ is the experimental buckling load of the flange element and P_{cr} is the critical buckling of the plain column, determined from tests. Therefore, the buckling load of the web and flange elements of a dimpled column section was determined as $P_{crw} = \beta_{wd}P_{cr}$ and $P_{crf} = \beta_{fd}P_{cr}$, respectively; where β_{wd} and β_{fd} are defined as above, and P_{cr} is the critical buckling load of the dimpled column, obtained from tests. This assumption is based on the fact that the dimpled column had the same nominal dimensions, area and original material as the plain column; and they were both tested under purely axial compression. This assumption was checked experimentally by comparing the buckling loads obtained from the calculations $P_{crw} = \beta_{wd}P_{cr}$ and from the tests. For example, in the test group 4, the dimpled columns had strain gauges attached (as shown in Figure 1); the experimental buckling load in the web of the dimpled column was determined using the average strain readings from the long strain gauge ($P_{crw} = \varepsilon_{crw}EA_w$). It showed that the difference between the two buckling loads was within 10%. Though this assumption could not be validated for every dimpled column due to the difficulty of affixing strain gauges on all the dimpled specimens, the consistency of results obtained on this basis seems to further justify such an assumption (results shown below).

The dimpled steel specimen has a complex geometry and its cross section is not flat but rather waved. The initial strain distribution through the cross section is non-uniform as a result of cold work produced by the dimpling process (Nguyen et al. 2011). An exact theoretical treatment of dimpled specimens for calculating buckling coefficient is, therefore, extremely difficult if not impossible. However, to further simplify the calculation for the buckling coefficient, it was assumed that the dimpled section element acts like a plain section element under purely axial compression. The dimpled web and flange elements deemed to have the widths b_w and b_f, respectively, and an "effective" thickness t similar to those of the plain web and flange elements. Thus, the buckling coefficients of the web and flange could be calculated from equations (1) and (2), in which the material and sectional properties are of the dimpled section.

Theoretical buckling and ultimate loads of plain columns

The test results were compared with the predicted values based on theoretical and semi-empirical methods. The comparison was only applied to the plain column since there is no simple method available to obtain the strength of the dimpled column. The theoretical elastic local buckling load was obtained using a Finite Strip Method (FSM) program namely CUFSM (Schafer and Adany 2006). The theoretical ultimate load of a section or its component elements in post buckling range was determined from theoretical and semi-empirical formulae developed based on the 'effective width' approach (von Karman et al. 1932, Winter 1947). Therefore the ultimate strength of a plain element is determined using the effective width method. They include the von Karman's theoretical formula for 'perfect' plate members (von Karman et al. 1932): $P_{mL}/P_y = (P_{cr}/P_y)^{1/2}$, and the semi-empirical formula for plate members with 'initial imperfections' (Winter 1947): $P_{mL}/P_y = (P_{cr}/P_y)^{1/2}[1 - 0.22(P_{cr}/P_y)^{1/2}]$. Where P_{cr} is the critical buckling load, P_{mL} is the ultimate load and P_y is the yield load.

Test results and validation

Test results

Table 2 shows the results of the column tests which include the critical buckling, ultimate and yield loads of the whole column sections, as presented in columns (3)–(5); buckling loads and coefficients of web and flange elements obtained from equations (1) and (2), as shown in columns (6)−(11). The yield load of a column section was calculated using the yield stress multiplied by the cross section area. The results for the repeated tests were all similar with a maximum difference of 8% for the ultimate load, hence demonstrating the repeatability of the test results.

Compared to the plain column specimens from the same groups, the buckling and ultimate loads in the dimpled column specimens were increased over a range between 9% and 33% (9–33%) and 8–26%, respectively. The yield strength was increased by 13−51% in the dimpled column specimens. The statistical results and paired student's t-tests show that there are significant differences between the strengths of the plain and dimpled column specimens. Enhancements in buckling and ultimate strengths were observed in the dimpled steel columns as a result of the plastic deformation developed throughout the dimpled sheet (Nguyen et al. 2011).

The mean values of buckling coefficient k together with their standard deviation (S.D.) for plain and dimpled specimens in each group were plotted against the

sectional ratio b_f/b_w and are shown in Figure 3(a). The buckling coefficients of dimpled column specimens are significantly higher than those of plain ones. Figure 3(b) shows the mean values of P_{mL}/P_y together with their S.D. plotted against $(P_y/P_{cr})^{1/2}$. There are no significant differences between the values of P_{mL}/P_y for plain and dimpled column specimens. The consistency of results obtained on the load reduction P_{mL}/P_y of the section seems to justify the assumption made previously about the distribution of local buckling load on the web and flange elements of plain and dimpled column sections.

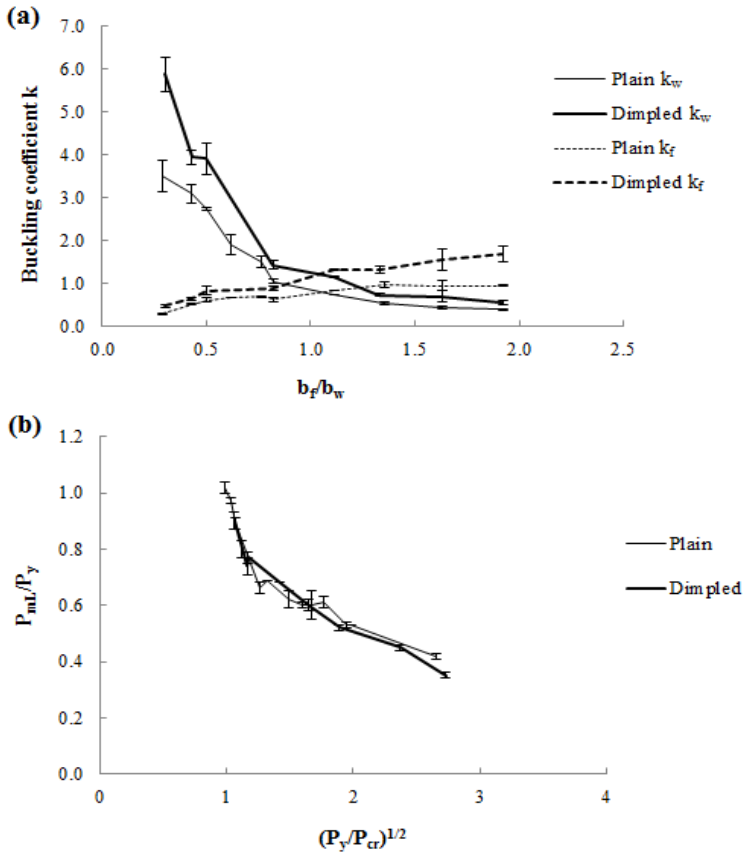

Figure 3 Test results (a) buckling coefficients for the plain and dimpled column specimens, and (b) graph of P_{mL}/P_y versus $(P_y/P_{cr})^{1/2}$ for the plain and dimpled column specimens; results presented as mean values and S.D. at data points.

Table 2 Column test results. The results derived on the basis of buckling of a whole section are presented in columns (3)−(5); the results derived on the basis of buckling of individual elements are presented in columns (6)−(11). [a] Buckling not measured by strain gauges.

Test group	Specimen	Section			Elements					
		Critical load	Ultimate load	Yield load	Critical load		Ratio		Buckling coefficient	
(1)	(2)	P_{cr} (kN) (3)	P_{mL} (kN) (4)	P_y (kN) (5)	P_{crw} (kN) (6)	P_{crf} (kN) (7)	β_w (8)	β_f (9)	k_w (10)	k_f (11)
1	P-T1.5F29.6W101.6L500#1	35.06	43.11	62.13	20.12	5.20	0.57	0.14	3.17	0.23
	P-T1.5F29.6W101.6L500#2	34.76	43.03	61.97	22.01	6.28	0.63	0.18	3.46	0.28
	P-T1.5F29.6W101.6L500#3	34.91	43.08	62.05	– a	–	–	–	–	–
	P-T1.5F29.6W101.6L500#4	34.84	43.06	62.01	–	–	–	–	–	–
2*	P-T0.9F15.0W44.7L200#1	14.94	14.94	14.21	10.10	3.05	0.78	0.22	3.24	0.28
	P-T0.9F15.0W44.7L200#2	14.88	14.88	14.40	12.18	3.30	0.88	0.22	3.77	0.30
	P-T0.9F15.0W44.7L200#3	14.56	14.56	14.36	–	–	–	–	–	–
	P-T0.9F15.0W44.7L200#4	14.37	14.37	14.37	–	–	–	–	–	–
	U-T0.9F15.0W44.7L200#1	16.49	16.49	21.87	13.74	3.73	0.83	0.22	5.63	0.46
	U-T0.9F15.0W44.7L200#2	17.82	17.82	21.30	14.85	4.03	0.83	0.22	6.32	0.52
	U-T0.9F15.0W44.7L200#3	17.80	17.80	22.11	14.83	4.02	0.83	0.22	6.09	0.50
	U-T0.9F15.0W44.7L200#4	17.26	17.26	21.26	14.38	3.90	0.83	0.22	5.48	0.45
3*	P-T1.5F30.4W70.0L500#1	44.28	46.19	48.15	–	–	–	–	–	–
	P-T1.5F30.4W70.0L500#2	44.30	45.80	47.22	–	–	–	–	–	–
	P-T1.5F30.4W70.0L500#3	44.29	46.00	47.26	25.09	9.81	0.57	0.22	2.94	0.50
	P-T1.5F30.4W70.0L500#4	44.29	46.00	47.02	26.88	9.99	0.61	0.23	3.25	0.52
	U-T1.5F30.4W70.0L500#1	46.91	48.30	65.34	28.47	10.64	0.59	0.22	4.16	0.68
	U-T1.5F30.4W70.0L500#2	49.58	52.38	66.69	30.09	11.25	0.59	0.22	3.93	0.65
	U-T1.5F30.4W70.0L500#3	48.25	50.34	64.12	29.29	10.94	0.59	0.22	3.84	0.62
	U-T1.5F30.4W70.0L500#4	48.25	50.34	66.41	29.29	10.94	0.59	0.22	3.84	0.62
4*	P-T1.0F50.8W101.6L500#1	6.20	20.49	50.64	–	–	–	–	–	–
	P-T1.0F50.8W101.6L500#2	7.84	21.24	50.28	–	–	–	–	–	–
	P-T1.0F50.8W101.6L500#3	7.25	21.46	50.56	3.73	1.58	0.54	0.23	2.77	0.59
	P-T1.0F50.8W101.6L500#4	7.27	21.38	50.24	3.51	1.69	0.48	0.23	2.71	0.65
	U-T1.0F50.8W101.6L500#1	8.24	23.19	65.27	4.21	1.79	0.51	0.23	3.73	0.79
	U-T1.0F50.8W101.6L500#2	9.97	23.29	65.22	5.09	2.17	0.51	0.23	4.41	0.98
	U-T1.0F50.8W101.6L500#3	8.20	22.21	65.45	4.19	1.78	0.51	0.23	3.60	0.75
	U-T1.0F50.8W101.6L500#4	8.80	22.90	65.31	4.49	1.92	0.51	0.23	3.91	0.84
5	P-T0.8F31.0W51.7L200#1	6.84	13.95	23.01	3.42	2.11	0.50	0.32	1.76	0.67
	P-T0.8F31.0W51.7L200#2	7.46	13.79	23.06	3.48	2.14	0.44	0.29	2.08	0.68
	P-T0.8F31.0W51.7L200#3	7.77	14.40	22.69	–	–	–	–	–	–
	P-T0.8F31.0W51.7L200#4	7.36	14.05	22.92	–	–	–	–	–	–
6	P-T0.8F38.0W51.7L200#1	6.78	14.94	25.96	3.13	1.77	0.46	0.23	1.61	0.69

	P-T0.8F38.0W51.7L200#2	6.27	14.92	26.00	2.74	1.78	0.40	0.28	1.41	0.71
	P-T0.8F38.0W51.7L200#3	6.90	14.66	25.92	–	–	–	–	–	–
	P-T0.8F38.0W51.7L200#4	6.65	14.84	25.96	–	–	–	–	–	–
7*	P-T1.2F24.5W32.0L200#1	21.10	22.23	25.59	10.61	7.54	0.48	0.36	1.02	0.60
	P-T1.2F24.5W32.0L200#2	23.39	23.39	25.61	11.37	8.36	0.49	0.36	1.09	0.66
	P-T1.2F24.5W32.0L200#3	22.80	23.25	25.52	–	–	–	–	–	–
	P-T1.2F24.5W32.0L200#4	22.46	22.46	25.75	–	–	–	–	–	–
	U-T1.2F24.5W32.0L200#1	25.81	26.04	28.82	12.31	9.22	0.49	0.36	1.40	0.86
	U-T1.2F24.5W32.0L200#2	26.92	26.92	29.32	12.84	9.62	0.49	0.36	1.55	0.95
	U-T1.2F24.5W32.0L200#3	25.89	25.89	28.74	12.35	9.25	0.49	0.36	1.45	0.89
	U-T1.2F24.5W32.0L200#4	24.61	25.30	29.48	11.74	8.79	0.49	0.36	1.33	0.82
8*	P-T1.2F32.5W32.0L400#1	19.48	20.42	30.77	7.63	7.83	0.39	0.40	0.74	0.84
	P-T1.2F32.5W32.0L400#2	21.46	21.46	30.88	7.69	7.94	0.37	0.38	0.74	0.85
	P-T1.2F32.5W32.0L400#3	18.48	19.90	30.89	–	–	–	–	–	–
	P-T1.2F32.5W32.0L400#4	18.50	19.90	30.53	–	–	–	–	–	–
	U-T1.2F32.5W32.0L400#1	25.81	25.81	35.23	9.82	9.98	0.38	0.39	1.16	1.31
	U-T1.2F32.5W32.0L400#2	24.32	24.32	34.78	9.25	9.40	0.38	0.39	1.14	1.29
	U-T1.2F32.5W32.0L400#3	26.31	26.31	34.79	10.01	10.17	0.38	0.39	1.17	1.33
	U-T1.2F32.5W32.0L400#4	26.80	26.80	34.96	10.19	10.36	0.38	0.39	1.16	1.31
9	P-T1.2F38.0W32.0L400#1	16.44	20.61	35.33	5.88	8.01	0.36	0.49	0.57	1.05
	P-T1.2F38.0W32.0L400#2	17.18	21.85	35.47	5.58	7.29	0.32	0.42	0.53	0.92
	P-T1.2F38.0W32.0L400#3	14.41	23.67	35.46	5.27	7.15	0.33	0.47	0.51	0.94
	P-T1.2F38.0W32.0L400#4	16.01	22.04	35.42	–	–	–	–	–	–
	U-T1.2F38.0W32.0L400#1	19.18	26.84	39.59	6.73	8.74	0.36	0.49	0.76	1.32
	U-T1.2F38.0W32.0L400#2	19.45	27.00	39.48	6.82	8.87	0.32	0.42	0.71	1.23
	U-T1.2F38.0W32.0L400#3	19.93	26.72	39.65	10.33	14.37	0.50	0.72	1.11	2.06
	U-T1.2F38.0W32.0L400#4	20.65	27.23	39.89	10.35	14.87	0.50	0.72	1.14	2.18
10	P-T1.2F46.0W32.0L400#1	15.11	21.96	40.34	4.09	6.09	0.28	0.42	0.39	0.96
	P-T1.2F46.0W32.0L400#2	13.86	22.96	40.00	4.37	6.76	0.26	0.49	0.42	1.06
	P-T1.2F46.0W32.0L400#3	14.54	26.44	40.51	4.89	5.28	0.33	0.36	0.47	0.84
	P-T1.2F46.0W32.0L400#4	14.60	24.55	40.29	–	–	–	–	–	–
	U-T1.2F46.0W32.0L400#1	16.69	27.09	45.74	4.61	7.60	0.28	0.42	0.51	1.37
	U-T1.2F46.0W32.0L400#2	16.91	26.78	45.71	5.10	7.70	0.26	0.49	0.73	1.80
	U-T1.2F46.0W32.0L400#3	18.13	28.16	45.93	6.17	6.59	0.33	0.36	0.83	1.46
	U-T1.2F46.0W32.0L400#4	15.61	28.69	45.65	5.54	5.67	0.33	0.36	0.73	1.21
11	P-T1.2F55.0W32.0L500#1	11.08	24.16	45.74	4.06	5.19	0.23	0.47	0.39	0.97
	P-T1.2F55.0W32.0L500#2	11.98	24.69	45.51	4.02	4.93	0.24	0.49	0.40	0.94
	P-T1.2F55.0W32.0L500#3	12.37	23.57	45.34	–	–	–	–	–	–
	P-T1.2F55.0W32.0L500#4	12.51	23.92	45.51	–	–	–	–	–	–
	U-T1.2F55.0W32.0L500#1	15.03	26.44	51.84	4.69	7.84	0.24	0.48	0.53	1.73
	U-T1.2F55.0W32.0L500#2	15.47	27.08	51.58	5.64	7.90	0.24	0.48	0.64	1.74
	U-T1.2F55.0W32.0L500#3	12.40	27.06	51.38	4.44	6.07	0.24	0.48	0.53	1.41
	U-T1.2F55.0W32.0L500#4	15.25	27.11	51.58	4.63	8.00	0.24	0.48	0.55	1.86

Comparison of experimental and predicted results

The comparison of buckling loads of the whole column sections was discussed in details in Nguyen et al. (2012). The buckling loads of the web and flange elements, predicted by FSM were compared with the test results and they are shown in Figure 4(a). In general, the theoretical and experimental values are in good agreement, with a maximum difference of 15% for 7 out of 11 test groups. The difference, however, could be as great as 21% for the web buckling in test groups 1 and 2, and 17% for the flange buckling in test groups 6 and 7. For these test groups, the theoretical local buckling loads were even greater than the full section yield loads. The main reason for this could be the fact that these columns buckled in an inelastic region while the theoretical local buckling loads were evaluated by means of elastic analysis.

Figure 4(b) shows a comparison of values of P_{mL}/P_y versus $(P_y/P_{cr})^{1/2}$ given by experimental results and theoretical formulae including von Karman (1932) and Winter (1947). The von Karman's formula provided conservative predictions of the experimental results, with a maximum difference of 12–17%. The Winter's semi-empirical formula, however, gave lower values than the experimental ones; the main reason is that it accounts for the effect of initial imperfections and it is derived on the basis of buckling of individual elements. The results presented in Figure 4(b), however, are derived on the basis of a complete section in which some elements initiate buckling while others restrain the buckling elements until the compression reaches a stage at which these elements would buckle naturally (Rhodes 2002).

Design of plain and dimpled channel columns

The design of plain and dimpled channel columns was developed on the basis of buckling and ultimate loads of individual elements. This study focused upon obtaining complete design equations for the strength of individual elements. The strength capacity of a whole section considered both the capacity of the web and flange element. Therefore this approach might be extended to apply for a general section shape since they contain component elements which can be considered as web or flange elements.

From the experimental results, relationships of k_w versus b_f/b_w, k_f versus b_f/b_w and P_{mL}/P_y versus $(P_y/P_{cr})^{1/2}$ for the web and flange elements of the plain and dimpled channel columns were formulated using regression analysis. A similar design approach to that suggested by Yiu and Pekoz (2006) was adopted for determining buckling formulae. A two-line approximation was formulated to determine k from the experimental data for plain and dimpled elements. Also,

relationships of P_{mL}/P_y versus $(P_y/P_{cr})^{1/2}$ were established using power function fits. Good agreement between the correlation curves and the experimental data were obtained (the regression coefficient $r^2 = 0.76–0.98$).

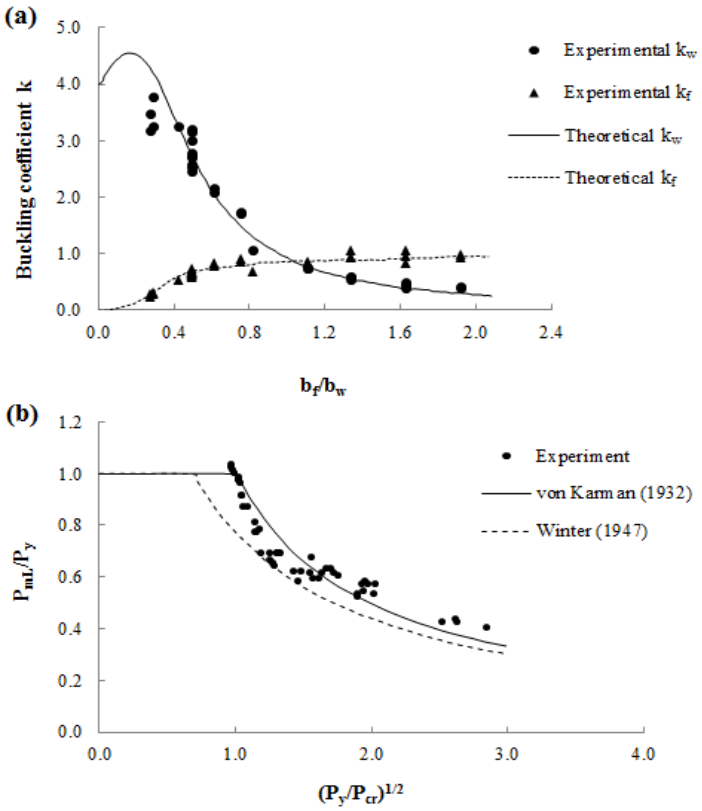

Figure 4 Comparison of the experimental and theoretical values for the plain column specimens (a) buckling coefficients, and (b) graph of P_{mL}/P_y versus P_y/P_{cr}; theoretical buckling values obtained by the FSM (Mulligan and Pekoz 1987).

All the design formulae can be summarised as follows:

Design formulae for determining buckling coefficients

For the web element of plain sections:

$k_w = -4.3682(b_f/b_w) + 4.7606$ $(r^2 = 0.94)$ $b_f/b_w \le 0.8659$ (3a)

$k_w = -0.6027(b_f/b_w) + 1.442$ $(r^2 = 0.86)$ $b_f/b_w > 0.8659$ (3b)

For the flange elements of plain sections:

$k_f = 1.6239(b_f/b_w) - 0.1902$ $(r^2 = 0.98)$ $b_f/b_w \le 0.5021$ (4a)

$k_f = 0.2903(b_f/b_w) + 0.4794$ $(r^2 = 0.76)$ $b_f/b_w > 0.5021$ (4b)

For the web element of dimpled sections:

$k_w = -8.1029(b_f/b_w) + 7.9649$ $(r^2 = 0.93)$ $b_f/b_w \le 0.8168$ (5a)

$k_w = -0.7777(b_f/b_w) + 1.9814$ $(r^2 = 0.85)$ $b_f/b_w > 0.8168$ (5b)

For the flange elements of dimpled sections:

$k_f = 1.7396(b_f/b_w) - 0.064$ $(r^2 = 0.86)$ $b_f/b_w \le 0.5048$ (6a)

$k_f = 0.6068(b_f/b_w) + 0.5078$ $(r^2 = 0.81)$ $b_f/b_w > 0.5048$ (6b)

Design formulae for determining ultimate strengths

For the web element of plain sections:

$P_{mL}/P_y = 0.828(P_{cr}/P_y)^{0.22}$ $(r^2 = 0.89)$ (7a)

For the flange elements of plain sections:

$P_{mL}/P_y = 0.863(P_{cr}/P_y)^{0.23}$ $(r^2 = 0.90)$ (7b)

For the web element of dimpled sections:

$P_{mL}/P_y = 0.758(P_{cr}/P_y)^{0.17}$ $(r^2 = 0.96)$ (8a)

For the flange elements dimpled sections:

$P_{mL}/P_y = 0.798(P_{cr}/P_y)^{0.20}$ $(r^2 = 0.97)$ (8b)

Table 3 shows an example of applying the design formulae and procedures for the column specimens in the test groups 10 and the obtained design values. The yield load was calculated as $P_{yw} = R_p A_w$ (9a) and $P_{yf} = R_p A_f$ (9b), where R_p is the yield stress determined from tensile test; A_w and A_f are the gross section areas of the web and flange elements, respectively. The buckling load P_{cr} and ultimate load P_{mL} of the whole column section were approximately calculated as $P_{cr} = P_{crw} + 2P_{crf}$ (10a) and $P_{mL} = P_{mLw} + 2P_{mLf}$ (10b). Compared to the column strengths measured in experiment (as presented in columns (3)−(4) in Table 2), the design buckling loads overestimated by 16% and 17% for the plain and dimpled specimens, respectively; the design ultimate loads differed by 13% and 1% for the plain and dimpled specimens, respectively. This indicates a good correlation between the design values and experimental results.

Table 3 Design values determined for the column specimens (the mean values of cross section dimensions and material properties of the four specimens in the group 10 were used).

Procedures	Parameters	Plain column		Dimpled column	
		Value	Equation	Value	Equation
(1)	(2)	(3)	(4)	(5)	(6)
Step 1	b_f/b_w	1.63		1.63	
Step 2	k_w	0.46	(3b)	0.71	(5a)
	k_f	0.95	(4b)	1.50	(6b)
Step 3	P_{crw}	4.76 (kN)	(1)	5.52 (kN)	(1)
	P_{crf}	6.05 (kN)	(2)	7.10 (kN)	(2)
Step 4	P_{yw}	9.02 (kN)	(9a)	9.35 (kN)	(9a)
	P_{yf}	14.71 (kN)	(9b)	15.52 (kN)	(9b)
	P_{crw}/P_{yw}	0.53		0.59	
	P_{crf}/P_{yf}	0.41		0.47	
Step 5	P_{mLw}	6.49 (kN)	(7a)	6.49 (kN)	(8a)
	P_{mLf}	10.35 (kN)	(7b)	10.44 (kN)	(8b)
Step 6	P_{cr}	16.85 (kN)	(10a)	19.73 (kN)	(10a)
	P_{mL}	27.19 (kN)	(10b)	27.37 (kN)	(10b)

Conclusions

The plain and dimpled channel columns, fixed at both ends, were successfully tested in purely axial compression. The test results were analysed to quantify the buckling and ultimate strengths of the whole section and its component elements. The experimental results were evaluated by comparing the buckling load with the theoretical buckling load obtained using the Finite Strip Method, and the ultimate load with the theoretical and semi-empirical formulae.

The column test results showed that the buckling and ultimate loads of the dimpled column specimens were significantly greater than plain column specimens originating from the same coil of material. It is clear that the cold work resulting from the dimpling process produces a significant increase in the strength of the dimpled column specimens.

It was observed that the local buckling loads predicted by the Finite Strip Method were in good agreement with experimental results, especially for the buckling of component elements. The ultimate loads predicted with the theoretical and semi-empirical formulae generally compared well with the experimental results. It was reasonable to assume that the compressive distribution of the critical buckling loads of the web and flange elements on the cross section of the dimpled column is similar to that of the plain column from the same test group. Based on the experimental results, design expressions for predicting the strength of plain and dimpled section under compression were

formulated. Though these design expressions were developed based on experimental data of channel columns, it can be generally applied to any sections since all cross sections can be considered of consisting of web or flange elements.

References

Bulson PS. The stability of flat plates. Chatto & Windus; 1970.

Coan JM. Large-deflection theory for plates with small initial curvature loaded in edge compression. ASCE: Journal of Applied Mechanics Division 1951;18:143-151.

Collins J, Castellucci MA, Pillinger I, Hartley P. The influence of tool design on the development of localised regions of plastic deformation in sheet metal formed products to improve structural performance. In: Proceedings of the 10th International Conference on Metal Forming. 2004. Paper no. 68.

Forest Products Laboratory. Methods of conducting buckling tests on plywood. Report no. 1554. United States Department of Agriculture, Madison, Wisconsin; 1946.

Mulligan GP, Pekoz T. Local buckling interaction in cold-formed columns. Journal of Structural Engineering 1987;113:604-620.

Nguyen VB, Wang CJ, Mynors DJ, English MA, Castellucci MA. Compression tests of cold-formed plain and dimpled steel columns. Journal of Constructional Steel Research 2012;69:20-29.

Nguyen VB, Wang CJ, Mynors DJ, English MA, Castellucci MA. Mechanical properties and structural behaviour of cold-rolled formed dimpled steel. Steel Research International 2011; Special Issue:1072-1077.

Rhodes J. Buckling of thin plates and members and early work on rectangular tubes. Thin-Walled Structures 2002;40:87-108.

Schafer BW, Adany S. Buckling analysis of cold-formed steel members using CUFSM: conventional and constrained finite strip methods. In: Proceedings of the 18th International Specialty Conference on Cold-Formed Steel Structures. 2006. p.39-54.

Venkataramaiah KR, Roorda J. Analysis of local plate buckling experimental data. In: Proceedings of the 4th International Specialty Conference on Cold-Formed Steel Structures. 1982. p.45-74.

von Karman T, Sechler EE, Donell LH. The strength of thin plates in compression. ASME: Transactions 1932;54:53-57.

Winter G. Strength of thin steel compression flanges. ASCE: Transactions 1947;112:527-554.

Yiu F, Pekoz T. Design of cold-formed steel channels. Research Report no. RP01-2. American Iron and Steel Institute; 2006.